JOURNAL OF SPACECRAFT AND ROCKETS
Vol. 43, No. 5, September–October 2006

Laser Window Design for the Army Hypersonic Compact Kinetic Energy Missile

Gerald Russell,* Stephen Cayson,† Mike Jones,‡ Wendy Carriger,‡ and Robert Mitchell‡
U.S. Army Aviation and Missile Research Development and Engineering Center, Redstone Arsenal, Alabama 35898
Forrest Strobel§ and Michael Rembert§
ITT Industries Advanced Engineering Sciences, Huntsville, Alabama 35806
and
Dave Gibson¶
Summit Research Corporation, Huntsville, Alabama 35802

The U.S. Army is currently developing the compact kinetic energy missile, which achieves hypersonic velocities at sea level. A state-of-the-art guidance technique called the side-scatter laser beam rider has been developed that utilizes a 1.06-μm laser to deliver an off-axis guidance link to the missile. Four rectangular side-looking optical windows are used on board the missile for the receivers. The peak flight velocity induces severe highly transient thermal gradients. To assess the effect of these gradients, detailed aerothermal and structural analysis followed by ground test experimental validation was conducted. The resulting window design utilized a Dynasil window (fused silica material fabricated by Meller Optics) along with Grafoil to constrain the window and eliminate gas paths to the laser receiver electronics as well as reduce dynamic effects with the metallic holder. The window design was then successfully validated during aerothermal testing conducted at the Naval Air Warfare Center T-Range Aerothermal Test Facility and ultimately flight-tested at Eglin Air Force Base. This paper will present a laser window design development process completed through flight testing to demonstrate window system performance.

Introduction

THE objective of the Compact Kinetic Energy Missile (CKEM) Laser Window Design Program was to develop and experimentally validate a laser window design for use in the CKEM hypersonic flight environment. The window design requirements included 1) accommodating the severe highly transient aeroheating and resulting thermal gradients; 2) providing an effective seal to prevent gas flow into the laser guidance electronics volume; 3) surface flush mounting to minimize aerodynamic loads; 4) minimizing dynamic effects on the window due to launch and flight shocks; and 5) providing an adequate surface finish and transmissibility for the laser wavelength of interest.

The Missile Guidance Directorate initially developed a conceptualized baseline design from which the final detailed design was derived. After completion of the final design, window specifications were developed, laser windows were purchased from Meller Optics, and attachment hardware was fabricated for use in ground and flight testing. Aerothermal tests were conducted at the Naval Air Warfare Center (NAWC) T-Range Aerothermal Test Facility, where heat fluxes and resulting thermal responses were simulated on the laser window design and attachment hardware to assess thermostructural performance and seal integrity. A final verification was performed during flight testing conducted at Eglin Air Force Base. This report documents the design and analysis of the laser window as well as the test and evaluation effort that validated and verified the laser window design.

Received 17 December 2004; revision received 18 June 2005; accepted for publication 10 July 2005.

*Senior Thermal Analyst, AMSRD-AMR-PS-PI; Gerald.russell@us.army.mil. Senior Member AIAA.
†Function Chief, AMSRD-AMR-SG-NC.
‡Senior Engineer, AMSRD-AMR-SG-NC.
§Senior Engineer, Advanced Engineering Sciences, 6767 Old Madison Pike, Suite 310.
¶Mechanical Engineer/Senior Designer, Engineering Development, 4910 Corporate Drive, NW.

Discussion

Geometry

Missile Configuration

The CKEM missile configuration is shown in Fig. 1. The current design essentially represents a test bed for state-of-the-art technology that includes guidance and control, propulsion, packaging of lethality mechanisms, thermal protection systems, and integrated system capability. The missile comprises a nose section, guidance section, and motor section. For the trajectory of interest, the missile nose and guidance sections are protected by a Chartek IV[1] thermal protection system, and the motor section utilizes a sacrificial overwrap of fiberglass epoxy. Chartek IV is a fiber-reinforced epoxy that has been utilized successfully in sea-level hypersonic sled test applications conducted at the Holloman High Speed Test Track. The fiberglass epoxy overwrap has been demonstrated in previous CKEM motor flight tests to provide sufficient thermal protection for short boost-phase periods. The window is located just forward of the transition from the ogive to the motor case cylinder. The local surface angle is approximately 6 deg for this region, with the distance from the nose tip being 18 in. (45.7 cm). The flight configuration and trajectory were used to design the ground test configuration to induce the same thermal gradients and peak temperatures and accurately assess the window design performance.

Window Configuration

The overall laser window configuration is provided in Fig. 2. Each region of interest is labeled and includes the laser window, Grafoil™ seal, restraint frame, reflector section, and detector housing. These components make up the laser window flight and ground test hardware. The unique Grafoil seal concept was developed by ITT Industries and represents a critical aspect of the design for limiting hot gas flow from reaching internal components. The Grafoil was also used to reduce stress by allowing expansion of the window and frame and to provide some level of dynamic isolation. The selected candidate window materials were polycrystalline aluminum oxynitride (ALON), sapphire, and fused silica (Dynasil™). These materials generally provide the highest performance in severe aerothermal

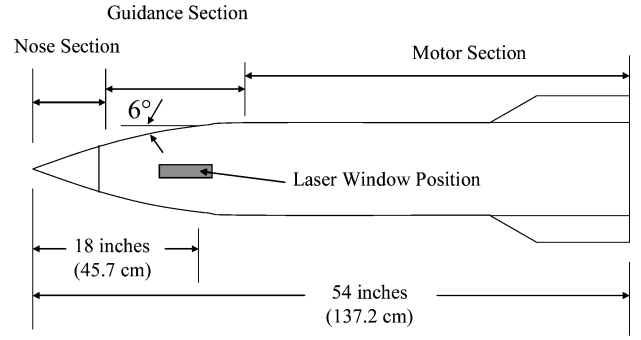

Fig. 1 CKEM missile configuration.

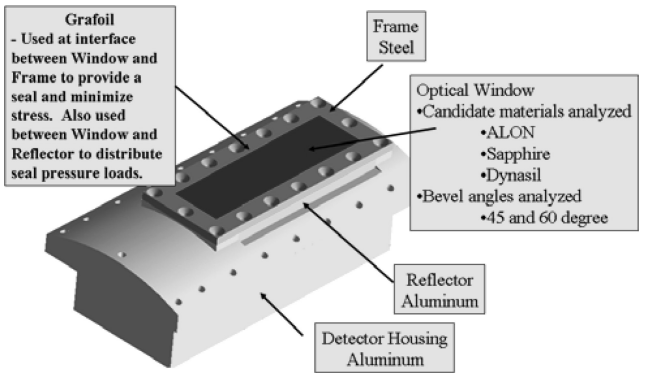

Fig. 2 Overall laser window hardware configuration.

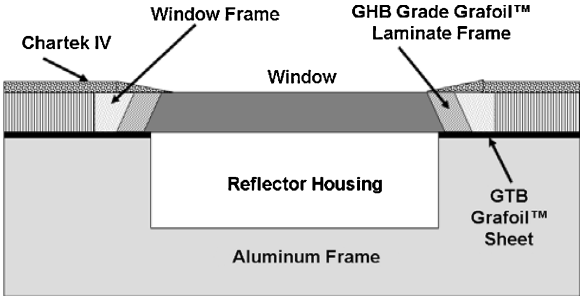

Fig. 3 Cross section of laser window attachment concept.

environments and were well suited for the initial studies for the CKEM application. Specific trades were conducted to assess thermal stress effects, which are generally the critical factor in the use of ceramics. The overall window dimensions were 0.88 in. (2.24 cm) wide × 2.89 in. (7.34 cm) long with a 0.1-in. (0.25-cm) wall thickness. Trades were performed for two bevel angles of 45 deg and 60 deg to reduce thermal stress and provide adequate surface contact with the Grafoil and steel attachment frame. As can be seen in Fig. 3, the Grafoil seal is positioned to eliminate any direct contact with the housing hardware and is compressed to ensure adequate seal under ambient and elevated temperatures. The Chartek IV heat shield is beveled into the flush mounted window to minimize flow disturbances.

T-Range Test Configuration

Figure 4 provides a view of the aerothermal ground test configuration conducted at the NAWC T-range facility. The test cone is assembled on to an instrumentation cylinder, which contains all instrumentation lines, and the cylinder attaches to the translation hardware for injection of the test samples after facility flow stabilization. A 1.35-in. (3.43-cm)-radius spherical steel nose tip was utilized along with a 0.05-in. (0.13-cm) Chartek IV heatshield to match the flight configuration. The test configuration also includes the attachment frame, seal, and window. The calorimeter cone was configured in the same geometry as the window test cone shown in Fig. 4, but is simply

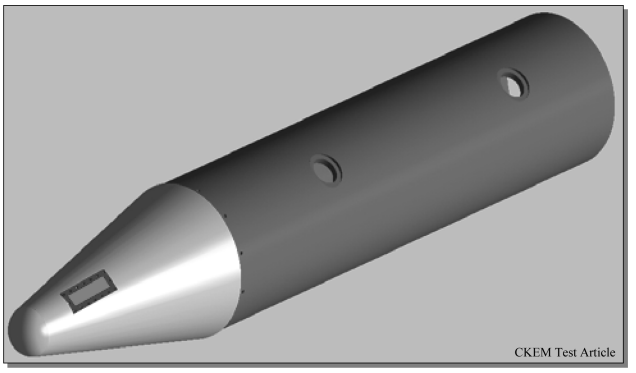

Fig. 4 T-range test sting and laser window test hardware.

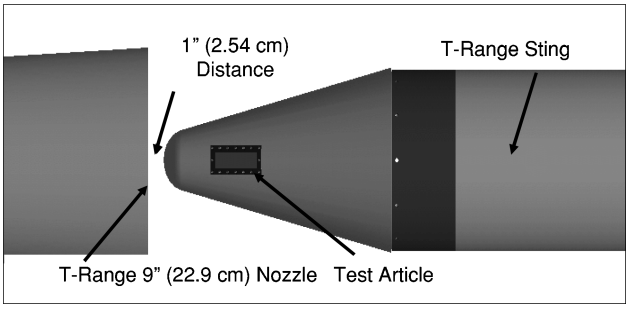

Fig. 5 Overall test configuration after injection.

composed of a solid stainless-steel cone and calorimeter plate attachment (in place of the window). The size of the spherical nose tip, distance from the nose tip, and cone angle were analytically selected to match flight environments for the specific window station during flight. The window was located approximately 4.5 in. (11.4 cm) from the nose tip. The calorimeter comprised a 0.06-in. (0.15-cm)-thick skin instrumented with four welded thermocouples to obtain a window location thermal response. Two static pressure gauges were also used to obtain pressure at the window location. These data were used to verify the flowfield conditions and aerothermal environment as well as to validate the analytic predictions that were subsequently used for flight predictions. In addition to the calorimeter cone instrumentation, a thermocouple and pressure transducer were located in the volume below the actual laser window hardware to measure any temperature or pressure increase within the laser receiver volume. Any significant rise in either of these measurements might indicate a seal leak allowing hot gas to enter the temperature-sensitive laser receiver volume. The holes in the instrumentation cylinder seen in Fig. 4 identify where the injection arms mount. This assembly was positioned outside the test rhombus (or region of uniform flow) aft of the nozzle until flow conditions stabilized. When flow conditions stabilized, the test sting was injected into the high-temperature flow and then withdrawn prior to facility shutdown. This eliminated the effects of start-up and shut-down shocks typically associated with aerothermal facilities.

Figure 5 provides an overall view of the test sting and nozzle exit. Initially the test sting was positioned in the center of the nozzle exit. However, through additional analysis, it was determined that an offset was required to ensure a uniform flowfield over the length of the window. A 9-in. (22.9-cm)-exit-diameter Mach 3 nozzle was used to deliver the desired conditions. A standoff from the exit plane of 1 in. (2.54 cm) was selected to minimize injection concerns with the nozzle hardware. These conditions and configurations provided the most uniform flow and matched the desired convective thermal environment predicted for flight.

Materials

The materials used in this design and test effort included the laser window material candidates, seal material, heat-shield material, nose tip, attachment hardware, and housing hardware.

Table 1 Room-temperature thermal properties

Material	Density, lbm/ft^3 (kg/m^3)	Thermal conductivity, Btu/ft · hr · °F (W/m · K)	Specific heat, Btu/lbm · °F (kJ/kg · K)	Thermal expansion, in./in. · °F (cm/cm · °C)	Young's modulus, Mpsi (GPa)	Poisson's ratio	Mean strength MOR[a], ksi (MPa)
Sapphire	248 (3973)	20 (35)	0.18 (754)	2.8×10^{-6} (5.0×10^{-6})	50 (345)	0.27	65.5 (452)
ALON	230 (3684)	7.2 (13)	0.18 (754)	3.2×10^{-6} (5.8×10^{-6})	47 (324)	0.24	54.3 (374)
Dynasil	137 (2195)	0.8 (1.4)	0.18 (754)	2.8×10^{-5} (5.0×10^{-6})	11 (76)	0.16	8.5 (59)
Grafoil	70 (1121)	3.0 (5.2)	0.17 (712)	1.5×10^{-5} (2.7×10^{-5})	0.029 (0.2)	0.3	0.01[b] (0.07)

[a]Modulus of rupture (MOR). [b]Compressive.

The material candidates for the laser window included sapphire, polycrystalline ALON, and Dynasil. Sapphire was the initial material of choice for the window based on its high temperature capability and strength. In general, sapphire is typically a first candidate for high-temperature applications until thermostructural analyses are performed that expose the thermal stress concerns typical of sapphire as well as concerns over directionally dependent properties impacting fabrication. ALON is another high-temperature optical material, but has less strength than sapphire, has a high thermal expansion coefficient, and is not as established in production. However, since the material is polycrystalline, homogeneous properties exist, and the material can easily be fabricated, reducing cost. While the fused silica has lower strength than ALON and sapphire, it is usable at very high temperatures due to its extremely low thermal expansion, and it experiences reduced thermal stress, making it the primary candidate for application in high-temperature environments. As a result of the use of the simplified rectangular flat configuration, the complexity of fabrication was reduced, and costs were approximately the same for each of the materials.

Stainless steel was used for the nose tip and window frame. Aluminum was used in the laser window reflector and housing. Grafoil was selected for the seal design due to its high temperature and compression capability. A prestress or compression on the seal was applied to maintain the leakproof volume and provide restraint for the window. Chartek IV was applied in a 0.05-in. (0.13-cm) thickness on the outside surface of the steel cone to limit cone thermal response as well as replicating the actual flight missile heatshield design on the fore cone.

The thermal and mechanical properties used for the window design and evaluation are provided in Table 1. Room temperature values are provided for comparison in the table. However, temperature-dependent properties were used for each of the materials where necessary. The window material properties were taken from Harris.[2] The Grafoil properties were taken from vendor data.

A primary concern for any optical material is the minimization of surface flaws to ensure a high probability of survival. To ensure an adequate window design was provided for transmissivity requirements, surface finish specifications were defined for polishing.

Because this laser guidance system flight demonstration program was conducted to verify the side-scatter laser beam rider (SSBR) technology as a technology demonstration effort, survivability in weather was not a requirement. However, it should be noted that weather survivability for a fielded system is a critical aspect of the design requirements and must be included early in the design. At these hypersonic velocities at sea-level conditions, weather encounters can be extremely severe. As a result, the laser window design must consider weather encounters and will likely result in a relocation of the window to aft sections of the missile that remain primarily parallel to the flow. Survivability of thermal stress as well as impact effects must be considered. Because fused silica has relatively low structural strength a new material trade study may be required unless the window can be adequately protected from particle impact.

Aerothermal Environments

Following the identification of the missile configuration of interest, it was necessary to define the aerothermal environments for which the window design must successfully function. Two flight trajectories were considered: a baseline trajectory imparting worst-case conditions, and the actual test flight trajectory imparting a reduced level of severity and considered the more realistic environment for the flight test program. The ground test environments consisted of T-range conditions determined to simulate the baseline or worst-case flight thermal response of the laser window. Actual test conditions generated by the test facility were somewhat less favorable than those for the baseline flight but sufficient to validate the window design for the projected test flight as well as identifying additional thermostructural capability. The aeroheating and thermal analysis code (ATAC3D)[3] was used to develop the transient aerothermal boundary conditions, which were then mapped onto the three-dimensional finite element analysis models to predict stresses, both thermal and pressure-induced.

The resulting aerothermal boundary conditions for the three test conditions of interest (baseline flight, actual test flight, and T-range test) are provided in Fig. 6–8. Figure 6 provides a comparison of recovery temperature with peaks on the order of 2000–2600°F

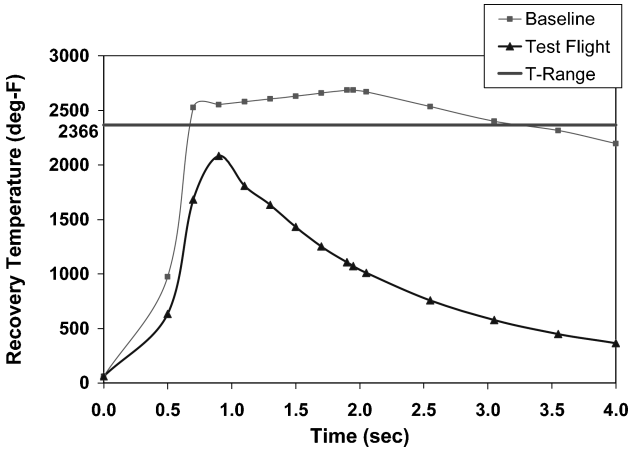

Fig. 6 Recovery temperature comparisons.

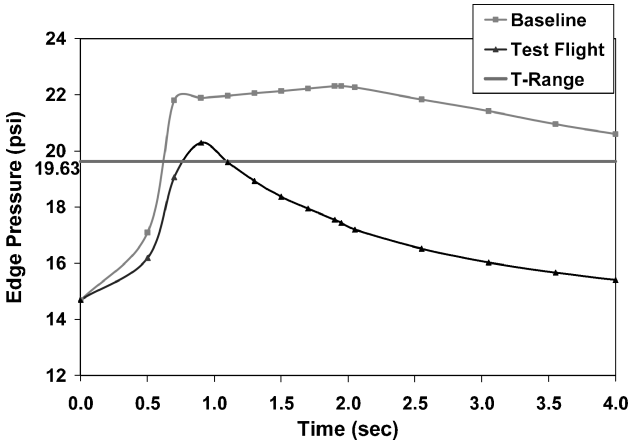

Fig. 7 Edge pressure comparisons.

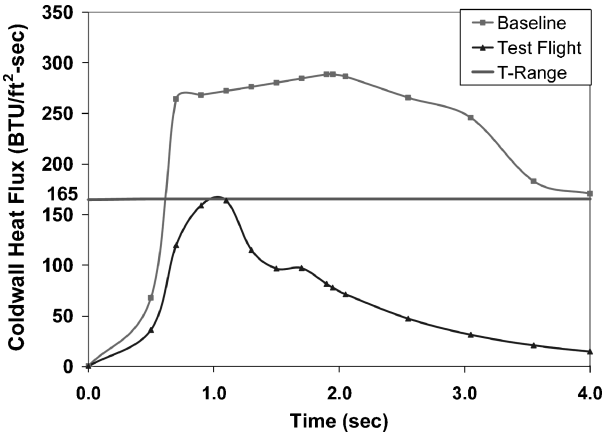

Fig. 8 Cold wall heat flux comparisons.

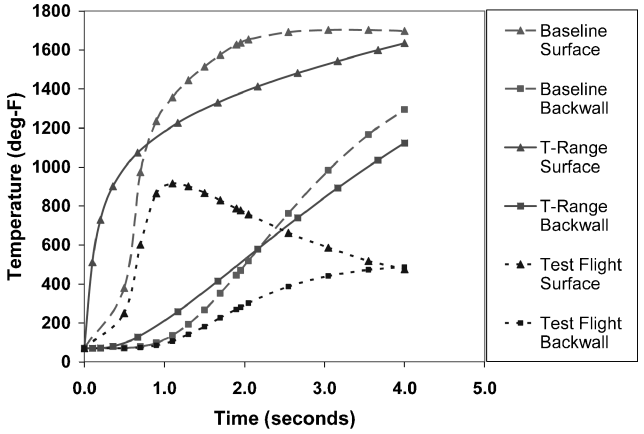

Fig. 9 ATAC3D predicted Dynasil window thermal response comparisons.

(1094–1427°C). Again, the main objective was to match or exceed the actual flight conditions, which reached a peak of only 2100°F (1149°C). Using a T-range condition of 2200–2300°F (1205–1260°C) provided a means of assessing additional capability in the design. The T-range conditional actually delivered was 2366°F (1297°C). The resulting edge pressure conditions, provided in Fig. 7, show relatively good agreement in pressure loads. However, the finite element analyses indicated that the stress response of the window design was dominated by thermal gradients, with pressure loads being negligible.

Figure 8 provides the resulting cold-wall heat fluxes for the various test conditions. The peak heat flux rate matches well between the actual projected flight and T-range conditions. However, the induced transient heat flux during the T-range ground test was considered more severe than the projected test flight condition in inducing thermal gradients and subsequent thermal stresses. The temperature response predictions from ATAC3D for the Dynasil window design are provided in Fig. 9 for the three conditions of interest. As can be seen, the T-range test conditions induce transient thermal gradients falling between the baseline flight and the actual projected test flight results. These results provided confidence of a validated flight design as well as providing an indication of additional higher velocity flight capability. The peak temperature and stress response during the actual test flight represents the criteria for selecting a T-range test period. The test time was selected to ensure that the peak stress experienced during the T-range test exceeded that seen for the actual test flight. The T-range induced thermal response is similar in magnitude to the thermal gradients experienced during the baseline flight, and far exceeds the actual test flight response.

Finite Element Analysis

Analyses were performed using the ATAC3D aerothermal analysis code to provide convective and pressure boundary conditions

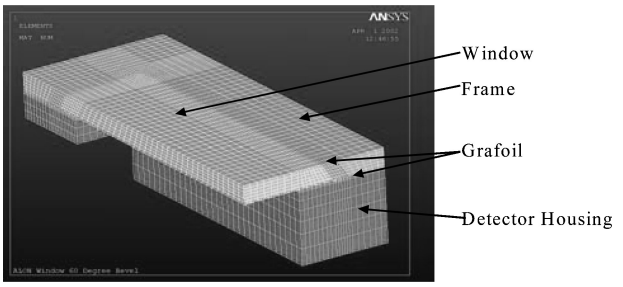

Fig. 10 ANSYS finite element analysis model.

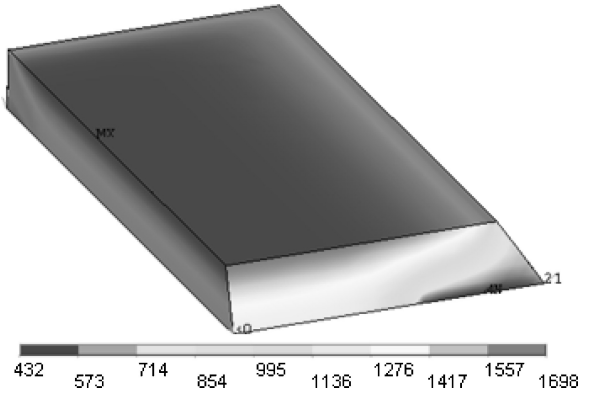

Fig. 11 Dynasil window peak thermal response contours (°F).

coupled with the ANSYS finite element analysis code to solve the three-dimensional finite element problem. Shown in Fig. 10 is the finite element analysis model of the window attachment design. Planes of symmetry were utilized to perform the analyses with the detector housing, window, seal, and frame included in the finite element model. The analytic model included transient temperature response, thermal expansion, and the appropriate constraints with respect to the remainder of the ogive assembly. The Grafoil seal was modeled with prestress loads of 500 psi (3.45 MPa) or 12.5% compression to ensure that an adequate seal at elevated temperature was maintained. This was accomplished through the use of analysis to define the displacement necessary to induce the appropriate compression. The window frame was designed to have an interference fit with the gasket. Upon installation, the torque required for the bolts was defined and the Grafoil gasket was compressed by the appropriate amount to properly seal the window. The Grafoil material used was supplied in sheets in the appropriate thickness to allow for compression and to maintain the outer mold line continuity. A device was developed to allow for the multiple angle cut required for the beveled window. Analysis was initially conducted assuming the baseline condition to assess the relative worst case thermal stress response. Figure 11 provides a representative thermal response contour for the Dynasil under the baseline conditions. The temperature contours are similar for the other window materials, with edge temperatures being lower due to attachment conduction. Fig. 12 provides the baseline condition thermal response histories for the sapphire and Dynasil windows at the center top and bottom locations of the window section. The thermal response results for Dynasil can be compared to the ATAC3D one-dimensional thermal response results shown in Fig 9. Very good agreement is achieved, verifying the temperature-dependent thermal boundary conditions calculated using ATAC3D. As can be seen, the Dynasil thermal response reaches 1600°F (871°C) rapidly and the backside thermal response approaches 1300°F (705°C) by the end of the flight. An example of the resulting stress contours for the baseline conditions is provided in Fig. 13 for the Dynasil window design. A complete comparison of stress results for the various materials and bevel configurations is provided in Table 2. Positive values represent tensile stress and negative values represent compressive stress. The table contains the tabularized peak temperature and tensile stress response comparison

Table 2 Thermostructural response comparison of tensile stress

Bevel		Peak surface temperature, °F (°C)	Backside temperature,°F (°C)	Peak stress, ksi (MPa)	Material strength MOR, ksi (MPa)	Margin of safety
45-deg	Sapphire	1250 (677)	1047 (564)	131 (900)	66 (452)	−
	ALON	1391 (755)	1093 (590)	95 (654)	54 (375)	−
	Dynasil	1709 (932)	1314 (712)	2.6 (18)	9 (59)	+
60-deg	Sapphire	1223 (662)	1020 (549)	115 (793)	66 (452)	−
	ALON	1385 (752)	1088 (587)	89 (617)	54 (375)	−
	Dynasil	1697 (925)	1293 (701)	26 (18)	9 (59)	+

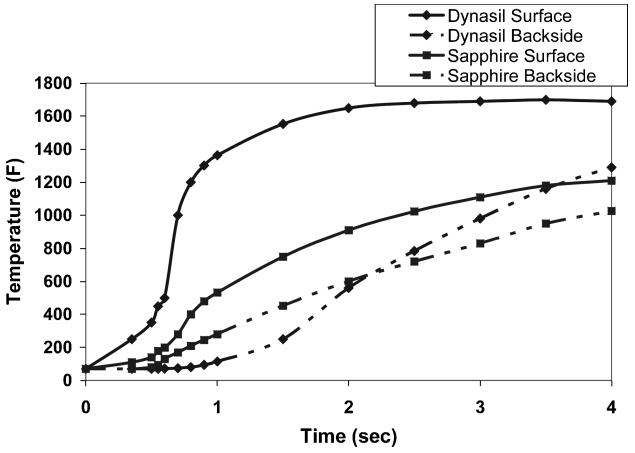

Fig. 12 Finite element analysis thermal response predictions.

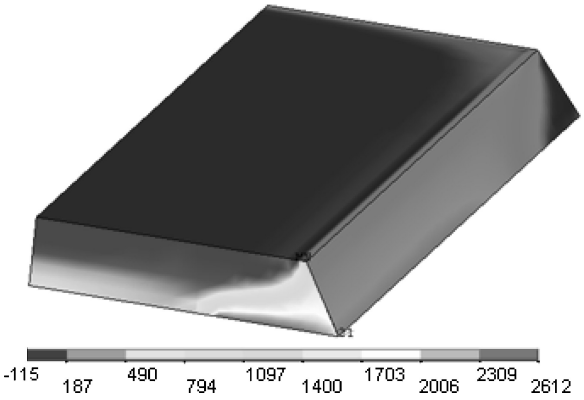

Fig. 13 Dynasil window peak stress prediction (psi).

for the three window designs, along with a comparison of bevel variation effects. Surface and backside temperature responses are provided for the three materials. As can be seen, larger thermal gradients are experienced for the Dynasil than are developed in the sapphire and ALON. However, considering the significant impact of thermal expansion properties, the resulting tensile stress levels for the sapphire and ALON far exceed their strength levels and clearly eliminate them for use in this application. The room temperature strength of sapphire is approximately 65.5 ksi (451 MPa), which is relatively high for optical materials. The ALON strength is also relatively high, at approximately 54.3 ksi (374 MPa), but less than that of sapphire. These strength values would suggest applicability to the CKEM environment. However, the thermal expansion properties of both sapphire and ALON result in exceedingly high thermal stress levels. The peak stress values for sapphire and ALON are 2 to 5 times greater than the materials' capability. The Dynasil peak stress is approximately 2.6 ksi (18 MPa), which is 20 to 25 times less than that for the sapphire and ALON designs, and 3 times less than the Dynasil structural capability. Based on these results, Dynasil provides the only solution that meets the CKEM flight requirements.

Figure 14 provides a comparison of the predicted tensile stress histories for the baseline and actual test flight conditions with two

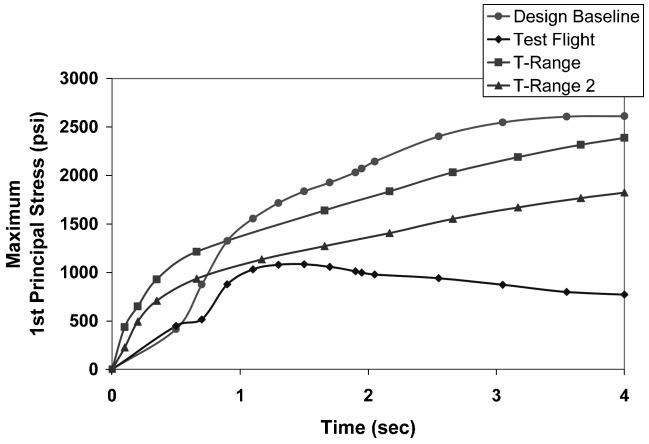

Fig. 14 Predicted baseline, flight, and T-range tensile stress levels for Dynasil.

T-range test conditions for Dynasil. These two test conditions were analyzed to determine the range of capability at T-range. As can be seen, the stress induced during the higher test condition [2366°F (1297°C) chamber temperature] matches well with the baseline flight peak stress response. Because the design qualification test objective was to meet the actual test flight requirements, a successful test condition would be to ensure that stress levels exceed the actual test flight stress. These two test conditions induce peak stress levels that clearly exceed the actual test flight induced stress. These results provide an indication of the range of conditions possible at T-range, to provide validation and qualification of the CKEM laser window design. It is interesting to note that the actual test flight-induced peak stress of approximately 1100 psi (7.6 MPa) occurs at approximately 1.2 s into the flight. The lower [2000 °F (1094°C):T-range] and higher [2366°F (1297°C):T-range] T-range test conditions reach approximately 1500 psi (10 MPa) and 1200 psi (8 MPa), respectively, in 1.2 s. To ensure added robustness in the verification test, a test period of 1.6 s was selected, which induced peak stresses between 1250 psi (9 MPa) and 1600 psi (11 MPa), depending on the resulting simulated test condition.

Test Results

T-Range Ground Test

As a result of the analytic conclusions for the window design effort, Dynasil was selected for fabrication and qualification testing, and a formal test plan was generated to provide test hardware drawings as well as required instrumentation specifications.[4] A variety of window fabrication houses were contacted and solicited for quotes to fabricate 10 windows having the optical surface finishing necessary to meet the laser receiver requirements. These requirements are less demanding than imaging requirements. The laser window only needs to pass the laser wavelength energy; stringent requirements for accurate imaging in the infrared are not necessary. Meller Optics was selected as the fabrication house for the windows with ground test and flight test hardware integration being conducted. Shown in Fig. 15 is an overview of the T-range test facility. The previously tested sting can be seen in the background with the injection table in the front view. The nozzle is located to the left of the test sting.

Fig. 15 Overview of T-range facility.

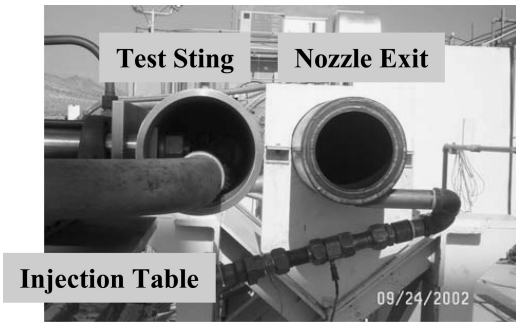

Fig. 16 T-range aft view of nozzle and injection sting.

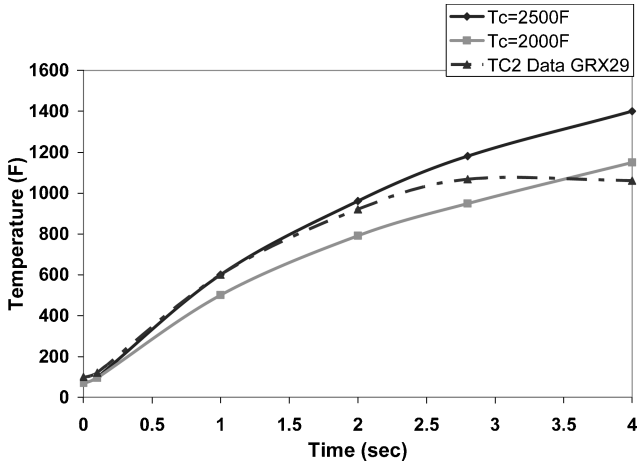

Fig. 17 Thin-skin backside thermal response predictions versus data.

Figure 16 provides an aft-looking forward view of the test section with the nozzle to the right. The test sting is translated out of the nozzle center for this view. Upon ignition of the burner and stabilized flow conditions, the test sting is translated into the nozzle flow. Real-time infrared imagery was obtained of the window during the test to verify thermal response and model validation. The initial week of testing at T-range involved the determination and verification of the necessary flow conditions to deliver the desired aerothermal heating environment. This effort required iterations on various flow parameters such as propane flow rate, air flow rate, burner temperatures, and flow meter checkout. The desired burner temperature and pressure conditions of 2366°F (1297°C) and 394 psi (3 MPa) were achieved, inducing worst-case thermal environments to the window design. After completion of the facility checkout runs, the calorimeter cone was tested to obtain edge pressure and thin-skin thermal response for the specific window location. The calorimeter runs were conducted and resulting data were compared to the predicted values. Figure 17 provides the measured backside thermal response of the steel thin skin for the calibration tests as compared to the predicted values. A peak temperature of approximately 1100°F (593°C) was achieved during the 2.7-s test period, which fell between the two test conditions considered. Additionally, the edge pressure measurements matched the predictions for 19–20 psi (131–137 kPa). These results provided confidence that the flowfield and resulting aerothermal environments were accurate and the actual window test could be performed. The laser window test configuration is shown in Fig. 18. The Chartek IV insulation is applied to the steel cone and faired into the window frame to minimize flow disturbances and simulate the actual flight test hardware. The Grafoil seal can be seen around the Dynasil window. The post-test view of the laser window and heat shield can be seen in Fig. 19. The window design successfully survived the severe aerothermal environment and resulting stress levels. Three tests were successfully conducted for the peak conditions to obtain repeatability. As a result of predicted stress levels being less than half of the documented available strength of Dynasil, Weibull modulus analysis was not conducted.

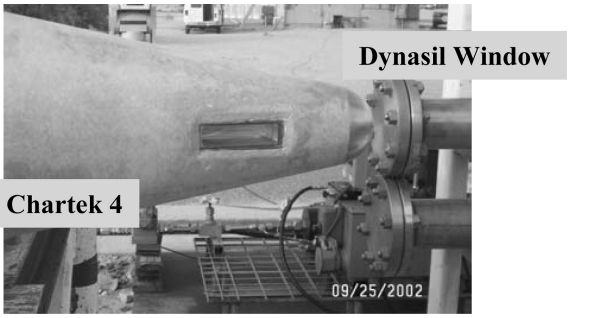

Fig. 18 Pretest cone configuration.

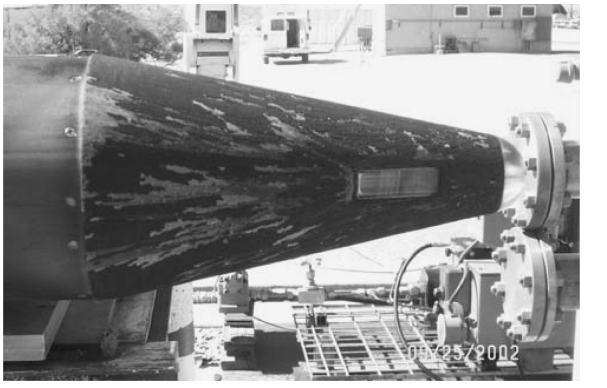

Fig. 19 Posttest cone response.

Figure 20 provides the infrared imaging thermal response for the test cone and window. The multiple blocked regions represent areas where thermal response was digitized. A variety of temperatures were collected for the window as well as the heat shield. The multiple window temperature measurements were taken in an attempt to identify possible gradients across the window along the centerline. Figure 21 provides the thermal response history of the window taken from the IR imaging data as compared with predictions. The initial hump in thermal response occurs during the injection period of the test. With the instantaneous exposure to conditions, the thermal rise rate is higher than that for the actual flight and can be considered a worst-case test. The window reaches a peak thermal response of approximately 1200°F (649°C) in 1.6 s. The resulting peak temperatures and thermal gradients for the test exceed the predicted thermal response of 900°F (482°C) in 1.0 s for the actual flight. The magnitude of thermal response is more in agreement with the baseline peak response of 1500°F (816°C) at 1.5 s and matches well with the predicted 1300°F (705°C) response for the higher T-range condition seen in Fig. 9. Because thermal expansion is the critical factor in the stress response, the test-induced thermal stress exceeds the actual flight stress and is near that achieved during the baseline flight. Based on these measured temperature responses, the laser window design

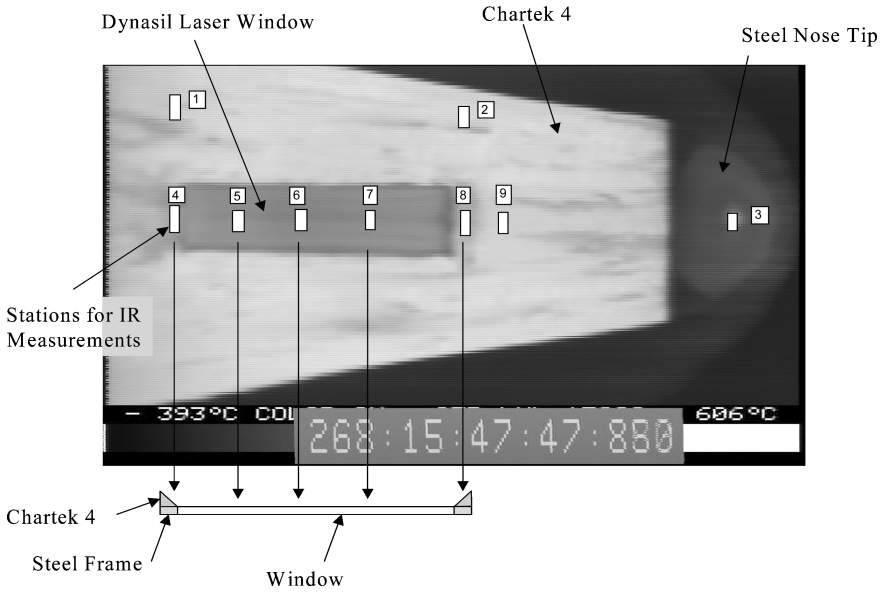

Fig. 20 IR image of laser window and heat shield near-peak response.

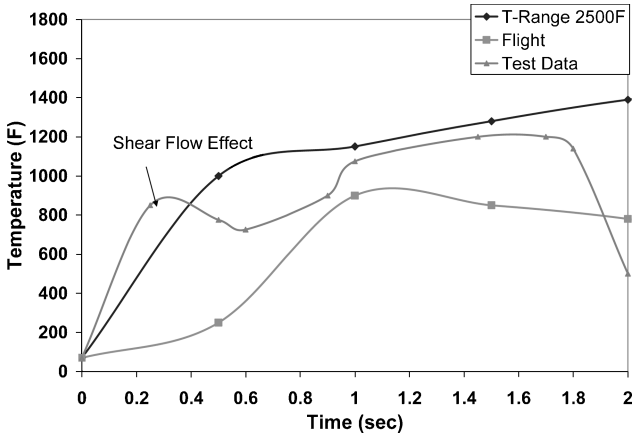

Fig. 21 Comparison of baseline, flight, and test data for window thermal response.

Fig. 22 Flight test of CKEM laser window configuration.

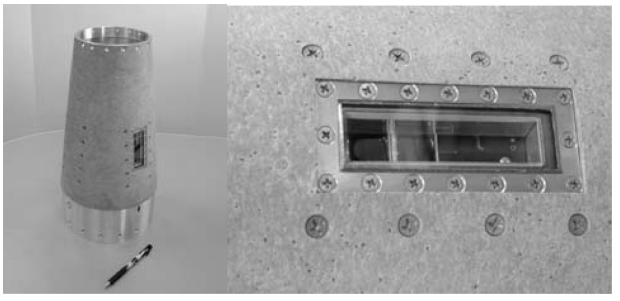

Fig. 23 Side-scatter beam rider flight hardware.

has been successfully validated and verified for the actual flight condition. The design has also been shown to provide additional capability for higher velocity flight.

Flight Tests

Figure 22 shows the launch of the CKEM Technology Demonstration Test (TDT-1) performed at Eglin Air Force Base, Florida, in August 2002. For TDT-1, only one window was mounted on the flight test vehicle. The laser window can be seen on the side of the missile ogive. The same laser window design configuration as validated during the ground test program was incorporated into the flight vehicle. The primary purpose of the test was to demonstrate a peak missile velocity in excess of Mach 4 so that a relevant flight environment could be created for the numerous experiments onboard the missile. These experiments included an isolation system for the missile inertial components, operation of the attitude control thrusters, and plume effects on guidance techniques. One of these guidance techniques was the side-scatter laser beam rider (SSBR). Photos of the SSBR flight test hardware are shown in Fig. 23. Unfortunately, a severe thrust misalignment present in the missile motor produced a flight path that did not intersect the SSBR laser guidance field, resulting in a "no-test" for this guidance link experiment. Although a similar experiment was conducted during a subsequent flight test (TDT-2), a telemetry failure and plume tracker anomaly produced another SSBR no-test. However, the most recent flight test (TDT-3), conducted in November 2004, resulted in a successful demonstration of this new off-axis beamrider guidance technique. Four laser windows were used for TDT-3 oriented 90-deg circumferentially around the missile. Specifically, the SSBR guidance link successfully communicated its two-axis spatially encoded guidance field to the missile during the boost phase of flight. Although the dynamic transmission characteristics of the four SSBR windows implemented for this flight cannot be quantitatively determined, throughout the flight each receiver acquired the appropriate spatially encoded guidance signals when the laser transmitter's

beam was positioned within its field of view. Postflight processing of the telemetry signals using a beam-decoding algorithm successfully produced missile positions for this period of flight. This is the first known flight test in which an off-axis beamrider guidance link was used to transfer missile to target (point-in-space) position updates to missile-borne receivers during flight using atmospheric scattering, instead of the usual direct communication path to aft-looking receivers. Additionally, it is known through analysis of the telemetry data that all four SSBR receivers were operational throughout the entire flight (>6 s), long after motor burnout and reduced plume signature caused the plume tracker used to point the guidance beam at the missile to lose track. This operability is ascertained by noting the increase in false detections associated with each receiver as the missile's roll position placed the sun in its field of view. The increase in false detections is owing to the sun-induced increase in shot noise at the individual receiver's output. Again, the exact transmission characteristics of the windows cannot be determined, but the structural integrity and basic operability of each window can be inferred from the data. As a result of the combined ground and flight tests, a total of 11 windows have been tested and through assessment of test data and recovered flight test hardware have been determined to have survived the relative ground test and flight environments.

Conclusions

A hypersonic laser guidance window technology has been developed and demonstrated for an Army missile system. The laser window design was developed and tested in a systematic process consisting of parametric and detailed analyses initially validated through multiple ground aerothermal tests under flightlike conditions. The final validation was completed during a flight test in which data were collected to verify the guidance signal received through the laser window during the flight time of interest. This program involved the concept of conducting design parametrics on a variety of materials for hypersonic window applications. The window design involved consideration of not only flight aerodynamic loads but, more importantly, the thermostructural response as a result of thermal gradients occurring within the material. Thermal gradients often dominate the structural response of hypersonic materials and can result in the use of materials having lower strength but reduced thermal gradients. The use of sound analytic methods and applicable ground aerothermal tests ensured a low risk for the flight test program used to demonstrate the laser guidance technology. The application of an uncooled optical window for hypersonic sea-level flight is unique and pushes the state of the art in window design technology.

Acknowledgments

The authors acknowledge the CKEM Program for funding the Laser Window Design, Test, and Evaluation Program in support of the AMRDEC research and development mission. The authors also extend sincere gratitude to Warren Jaul and his support team at the Naval Air Warfare Center T-Range Aerothermal Test Facility for their outstanding efforts in conducting the test to obtain the critical window design validation data. Additional appreciation is acknowledged for Mellor Optics in fabricating and delivering to an accelerated schedule the window hardware needed to meet the ground test and flight test schedules.

References

[1]Russell, G. W., "Investigation of Thermal Performance of an Epoxy Composite Using a Complex Charring Model," AIAA Paper 96-2776, June 1996.

[2]Harris, Daniel, C., *Materials for Infrared Windows and Domes*, SPIE Optical Engineering Press, Bellingham, WA, 1999, pp. 391–402.

[3]Murray, A. L., and Russell, G. W., "Coupled Aeroheating/Ablation Analysis for Missile Configurations," *Journal of Spacecraft and Rockets*, Vol. 39, No. 4, 2002, pp. 501–508.

[4]Russell, G. W., Strobel, F. A., Rembert, M., Cayson, S., Jones, M., Carriger, W., Mitchell, R., and Gibson, D., "Army Hypersonic Compact Kinetic Energy Missile Laser Window Design," *Proceedings of the International Society for Optical Engineering*, *Window and Dome Technologies VIII*, Vol. 5078, 2003, pp. 28–39.

T. Lin
Associate Editor